

## Gamma – Ray Spectroscopy: Effect of Strength and Distance on the Performance of a Detector

Godwin Bassey EKONG<sup>1</sup> and Bako Nyikun AUDU<sup>2</sup>

<sup>1</sup>Nigerian Nuclear Regulatory Authority, Abuja, <sup>2</sup>Physics Dept., Taraba State University, Jalingo.

<sup>1</sup>godwin.ekong@nnra.gov.ng, <sup>2</sup>b.n.audu@tsuniversity.edu.ng

**Abstract:** Gamma-ray spectroscopy of gamma sources were studied using High-Purity Germanium (HPGe) semiconductor detector in this experiment. The spectra produced by <sup>137</sup>Cs, <sup>60</sup>Co, <sup>152</sup>Eu and unknown sources were used in evaluating the performance of the detector as regarding its efficiency, energy resolution, and ability to analyse complex spectra as well as characteristics of the source spectra. The efficiencies on two limits of energy photon was determined to be  $(0.20 \pm 0.00)\%$  at 662keV to  $(0.11 \pm 0.01)\%$  at 1332keV for Absolute Peak Efficiency ( $\epsilon_{ap}$ ),  $(29.3 \pm 0.00)\%$  at 662keV to  $(15.9 \pm 0.01)\%$  at 1332keV for Intrinsic Peak Efficiency ( $\epsilon_{ip}$ ), and  $(0.09 \pm 6E^{-5})\%$  at 662keV to  $(0.14 \pm 3E^{-4})\%$  at 1332keV for Absolute Total Efficiency which were as expected. The linearity energy response ratio of 1.5% at 662keV and 0.2% at 1332keV were determined between MCA and eye inspection. Energy resolution of the detector under study was  $(0.2 \pm 0.1)\%$  at range of 662 to 1332keV which was quite good when compared to standard data with gradient of  $-(0.6 \pm 0.8)$  when a graph of LogE versus LogR was plotted making it possible to analyze complex spectra from the unknown given source with clarity which is the proof the hallmark of Ge detector that gave it an edge over other detectors used for gamma spectroscopy.

### Introduction

Radioactive element of higher energy nuclei usually decay to nuclei of lower energy thereby producing gamma rays of various energies and intensities. Gamma-ray spectroscopy system is therefore the powerful technique for collection, quantifying and analysing or studying of gamma-ray energy spectrum produced by these radioactive elements (Slack and Way, 1959). Also, it can provide information on both energy and intensity of radiation emitted from a source of gamma ray or energetic x-rays (Heath, 1964). And the accuracy of this method has been proven with three known source samples, Cobalt-60, Sodium-22, and Cesium-137 (Slack et al, 1959). The major characteristic features produced by gamma-ray energy spectrum are: Photopeak or full energy peak, Compton continuum, Compton edge, Backscatter peak and characteristic x-ray peak. Photopeak or full energy peak corresponds to that interaction which the entire energy

of the incident photons is deposited in the detector. Compton continuum corresponds to Compton scattering events due to the partial energy deposition on the detector. Compton edge corresponds to the maximum energy that can be transferred to the recoil electron by a single scattering event. Backscatter peak result from the x-ray backscattered by surrounding material through a large angle of 180 back to the detector. Also, there exists other characteristic x-ray peak that is produced when the detector is closely surrounded by shielding material in which incident photon interacts (Knoll, 2010, Lilley, 2001 and Surrey, 2011).

These interactions are in different ways namely: Photoelectric effect, Compton scattering, and pair production. Photoelectric effect is predominantly with the energy range of 100KeV – 500KeV which involves the interaction between a photon and absorber atom in which the photon completely disappears and a tightly bound electron is ejected from the nucleus

of an atom. Compton scattering is with the energy range of 100KeV – 1.0MeV which involves the interaction of a photon with a free electron resulting in the scattering and the loss of energy by the photon and gain in energy by the recoil electron and thereby depositing partial photon energy on the detector. Lastly, pair production is with the energy above  $\sim 1.02\text{MeV}$  which is a coulomb type of interaction and occur when an incident photon interact in the electric field of the surrounding nucleus resulting in the formation of electron pairs (Knoll, 2010, Lilley, 2001 and Surrey, 2011). The way the resulting electron interacts with the detector material determines the mode of operation of the detector. In this experiment, High-Purity Germanium (HPGe) semiconductor detector was used to study these interactions.

HPGe semiconductor detector incorporates Germanium having impurity level as low as  $10^9 - 10^{10} \text{ atoms cm}^{-3}$  and a crystal diode

which when a high voltage reverse bias is applied behaves as a solid state ionisation chamber. It is highly desirable for many applications for analysing complex spectra when compared to those of scintillating detectors like the NaI (TI) although highly expensive (Knoll, 2010, Lilley, 2001 and Surrey, 2011). One reason for its analysis is the difference in statistical variation on critical number of events which determined the signal size in each case (Lilley, 2001). However, HPGe has to be cooled with liquid nitrogen at about temperature of 77K in order to stop thermal excitation which may result in high energy gaps that will have negative impact on the energy resolution (Knoll, 2010, Surrey, 2011).. The detector shall be used in this experiment to demonstrate the performance of modern gamma ray spectroscopy system as regarding, Energy calibration, energy resolution and ability to analyse complex spectrum.

### Experimental Set-up and Theory

The Energy calibration, energy resolution and ability to analyse complex spectrum are all dependent on the energy of the incident radiation deposited on the detector and the direct proportionality between this event and the when plotted result in obtaining energy calibration of the detector (Surrey, 2011). The energy resolution (R) measures the ability of the detector to resolve small differences in the energy of the incident  $\gamma$ -rays. Mathematically, this can be defined as

$$R = \frac{FMHW}{H_0} \times 100\% \quad (1)$$

Where *FMHW* is fullwidth of the full-energy peak at Half Maximum height, expressed in the number of channels, and  $H_0$  is the channel number corresponding to the centroid of the peak. Peak broadening can result in several sources, but by far the most important cause is due to statistical

fluctuations in a number of charge carriers produced by the detector in the event of identical energy deposition and if such fluctuations are characterised by poisson statistics, FWHM is expressed as (Heath, 1964):

$$R \propto E_\gamma^{-1/2} \quad (2)$$

Where  $E_\gamma$  is the peak energy. Taking log of both sides of the equation, the above equation becomes:

$$\log_{10} R = \log_{10} Q - \frac{1}{2} \log_{10} E_\gamma \quad (3)$$

Where Q is the constant of proportionality and a gradient of  $\frac{1}{2}$  (0.5) obtained from a plot of LogE (energy of gamma ray) versus LogR (detector resolution) implies that a poisson statistics is obeyed (Surrey, 2011). When considering a detector for any special application, the efficiency with which the photons may be detected is of major essence. The efficiency can be defined in terms of Absolute Total

**Gamma - Ray Spectroscopy...**

Efficiency ( $\epsilon_t$ ), Intrinsic Photo peak Efficiency ( $\epsilon_p$ ), and Intrinsic Total Efficiency ( $\epsilon_i$ ). Each case of the mentioned efficiency requires a precise knowledge of the source activity.  $\epsilon_t$  is dependent on counting geometry hence it's direct dependence on absolute disintegration rate (surrey, 2011). The equation can be defined as:

$$\epsilon_t = \frac{C_t}{N_\gamma} \times 100\% \quad (4)$$

Where  $C_t$  is the number of counts recorded per unit time of disintegration over a whole recorded spectrum,  $N_\gamma$  is the number of gamma quanta emitted by the source per unit time [7] which can also be defined as

$$N_\gamma = D_s I_\gamma(E_\gamma) \quad (5)$$

Where  $D_s$  and  $I_\gamma(E_\gamma)$  are rate of disintegration of the source and fraction number of gamma emitted per disintegration { Cs-137=0.85, Co - 60 = 2 } respectively. The  $\epsilon_i$  is independent of the counting geometry but dependent on detector properties. This can be defined by the expression below:

$$\epsilon_i = \frac{C_t}{N'_\gamma} \times 100\% \quad (6)$$

Where  $N'_\gamma$  is the total number of gamma-rays incident on the detector (Surrey, 2011),

$$N'_\gamma = \frac{\Omega}{4\pi} N_\gamma \quad (7)$$

Where  $\Omega$  is the solid angle subtended by the detector crystal at the point source.  $\epsilon_p$  is expressed as

$$\epsilon_p = \frac{C_p}{N''_\gamma} \times 100\% \quad (8)$$

$C_p$  is the net number of the photo peak which corresponds to the energy ( $E_\gamma$ ) emitted per disintegration and  $N''_\gamma$  is the total number of gamma quanta of energy which falls on the detector crystal and given by the expression below

$$N''_\gamma = \frac{\Omega}{4\pi} N'_\gamma \quad (9)$$

The gamma-ray spectrum produced by the gamma sources shall be used in evaluating the performance of the detector as regarding its efficiency, energy resolution, and ability to analyse complex spectra as well as characteristics of the source spectrum. The linearity energy response between MCA and eye inspection shall also be determined and the ability to analyse complex spectrum using the acquired knowledge of gamma spectroscopy shall be used. The experimental arrangement was as diagrammatically presented in Figure 1 with names and model numbers of each equipment well specified.

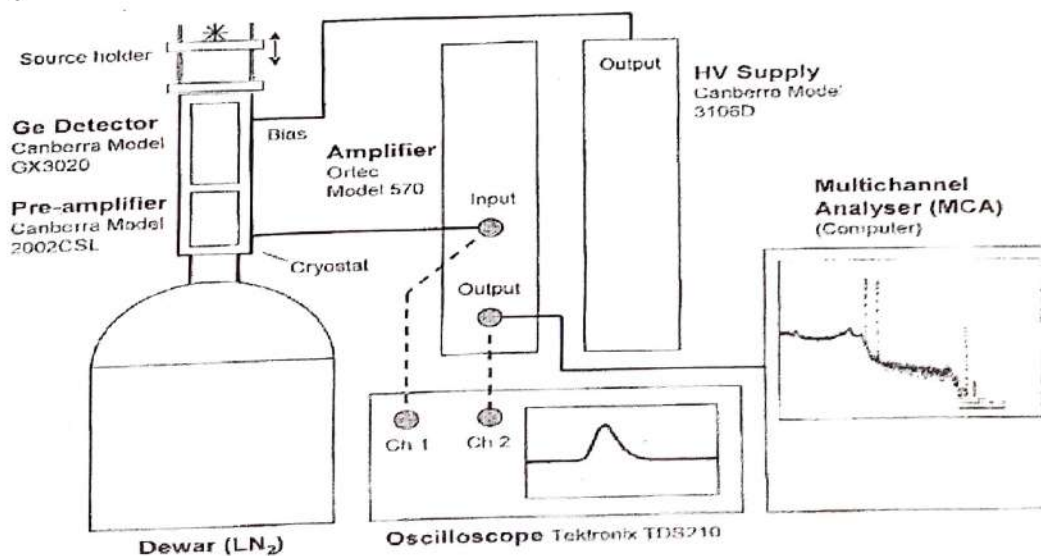


*Figure 1. Set up for gamma ray spectroscopy using HPGe detector [5]*

Source - detector distance was measured to be 180mm but was always adjustable to suit with desired result while the diameter of the detector crystal window was measured to be 60mm (Radius = 30mm). A sealed source of  $^{137}\text{Cs}$  was placed in the HPGe detector without any shield around it and a pre-set time of 300s was set up for the MCA in order to obtain a good statistical presentation of the spectrum. Acquisition of the spectrum was done on the MCA over that pre-set time for  $^{137}\text{Cs}$  and the same process was repeated for  $^{60}\text{Co}$  source. The acquired spectrum had characteristic features which were further studied. With the pre-set time remaining constant the gain of the pre-amplifier was increased to 100 and thereafter the  $^{60}\text{Co}$  source was taken very close to the detector and the spectra were obtained.

### Detector Characterisation and Energy Calibration

In this experiment, the detector was returned back to standard operating conditions and different sources with their corresponding energies were used: Cs-137 (662KeV), Co-60 (1173 and 1332KeV). The spectrum of each source was collected and the central channel of the full energy peak by eye inspection and by means of MCA was determined. The graph of central channel number versus energy in both cases was plotted. All the sources were further placed in front of the detector at the same ensuring that the dead time is not above 10% and this was used to calibrate the MCA. The peak search was conducted and full energy peak central channel, peak energy and FWHM were recorded. The information above was used to determine Energy Resolution from which a graph of Log R versus Log  $E_\gamma$  was further plotted and gradient determined from the graph. The Cs-137 was placed in the detector and a spectrum was obtained

over a pre-set time of 300s. A region of interest (ROI) over the entire spectrum was determined and total number of counts integrated per unit time over the whole spectrum was recorded ( $C_t$ ) and net number of count in a photo peak corresponding to the energy emitted ( $C_p$ ) was also recorded after stripping off that of the background which was earlier determined. The same procedure was repeated using Co-60 source. These values were used in calculating Absolute Total Efficiency ( $\epsilon_t$ ), Intrinsic Photopeak Efficiency ( $\epsilon_p$ ), and Intrinsic Total Efficiency ( $\epsilon_i$ ) while also taking note of the current activities.

The spectrum of Cs-137 (662KeV), Co-60 (1173 and 1332KeV) sources were acquired. The central channels of the full energy peak by eye inspection and by means of MCA were determined. The graph of channel number versus energy was plotted in both cases (see Figures 2a and b).

### Interpretation of Gamma spectra

Eu-152 source was placed in front of the detector to obtain energy range of 122keV to 1458keV. The resulting spectrum was to be used in determining the effectiveness of the detector in analysing complex spectra, then, a gamma-ray spectrum emitted from an unknown source was acquired by placing the unknown source in front of the detector window, with the knowledge of spectroscopy; the spectrum obtained from the experiment was used to identify the source. The spectrum of gamma ray emitted from  $^{137}\text{Cs}$  and  $^{60}\text{Co}$  were acquired as shown in Figure 2,3,7,8 and 9 and all the characteristic features were observed. These characteristic features correspond to those described earlier in the introduction. With the pre-set time remaining at 100s and as the  $^{60}\text{Co}$  source was taken very close to the detector an additional peak of 2505.7KeV was obtained (see Figure 8 and 9).

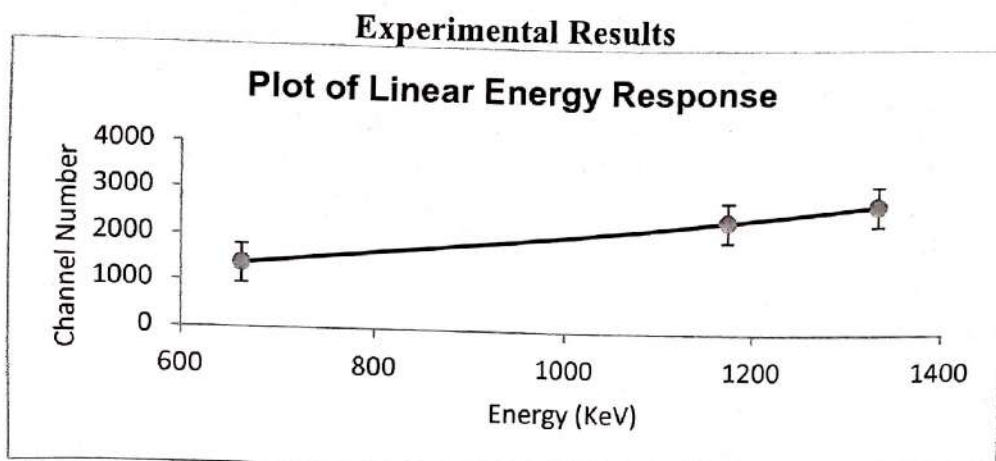


**Figure 2a:** Eye Inspection for source - detector distance of 200mm and 239930Bq for  $^{137}\text{Cs}$  & 20419.9Bq for  $^{60}\text{Co}$ . The error bars on the graph represent the all associated events of gamma yield and source-detector distance activity playing during the experiment.

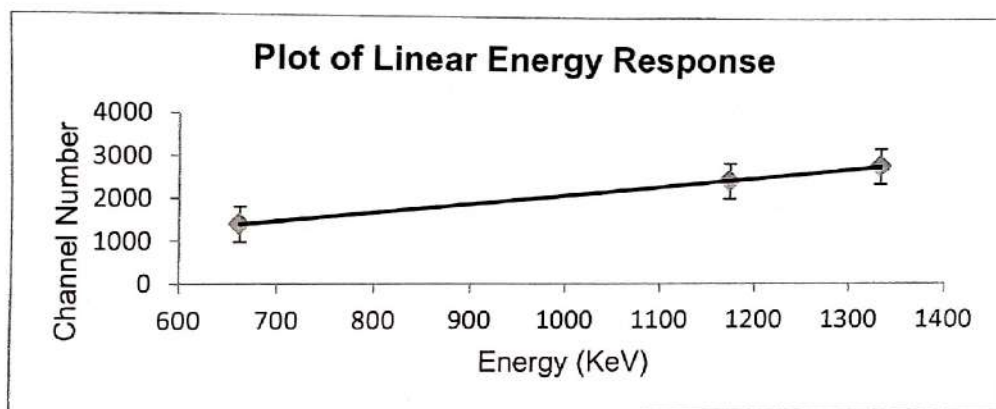


**Figure 2b:** MCA for source - detector distance of 200mm and 239930Bq for  $^{137}\text{Cs}$  & 20419.9Bq for  $^{60}\text{Co}$ . The error bars on the graph represent the all associated events of gamma yield, source-detector distance activity playing during the experiment.

The linearity energy response ratio between MCA and Eye inspection was 1.5% at 662KeV and 0.2% at 1332KeV

### Energy Resolution

Energy resolution of the detector under study was calculated to be  $(0.2 \pm 0.1) \%$  at a range of both 662KeV and 1332KeV using equation 1.(Figure 5).

### Detection Efficiency and Complex radiation spectra

The Absolute Total, Intrinsic Photo peak and Intrinsic Total efficiencies of the detector were determined using equation 4,6 and 8 with sources information from the spectra obtained and geometry of the detector with the sources current activities. Values ranging from  $(0.20 \pm 0.00) \%$  at

662KeV to  $(0.11 \pm 0.01) \%$  at 1332KeV was calculated for Absolute Peak Efficiency ( $\epsilon_{ap}$ ),  $(29.3 \pm 0.00) \%$  at 662KeV to  $(16.0 \pm 0.01) \%$  at 1332KeV for Intrinsic Peak Efficiency ( $\epsilon_{ip}$ ), and  $(0.09 \pm 6E^{-5}) \%$  at 662KeV to  $(0.14 \pm 3E^{-4}) \%$  at 1332KeV for Absolute Total Efficiency ( $\epsilon_{at}$ ) (see table 2, appendix). The graph of the efficiencies (%) versus Energy (KeV) was plotted (Figure 6a, b and c). Figure 10(Appendix) shows the energy spectrum of Eu-152 source which exhibited complex spectra. This source emits gamma ray energy of 122 to 1458KeV. Also, Figure 11 shows

**Gamma – Ray Spectroscopy...**

the energy spectrum of gamma-ray emitted from an unknown source.

**Discussion and Conclusion.**

Gamma-ray spectroscopy of some known and unknown source which emitted gamma radiation were study by the use of High-Purity Germanium (HPGe) semiconductor detector and the spectrum produced were used in evaluating the performance of the detector. Figures 3 and 7 show all the labelled characteristic features of Backscatter, Compton continuum, Compton edge as explained earlier for Cs – 137 at peak energy of 662 KeV. Cs-137 decay, has Ba  $K\alpha$ - X-rays in the region of 31 to 38 keV or precisely at 32.1keV and Pb  $K\alpha$ - shell X-ray at 74.2KeV

respectively that arose from internal conversion of the 662KeV transition. This internal conversion occurs when the transition energy between two energy levels is communicated directly to one of the surrounding orbital electrons causing it to be ejected from the atom (Ellis, 2007, Surrey, 2011). The geometry of the Ge detector does not have any attenuating material, other than air, between the source and the detector. It was however observed that small X-ray peaks were observed with low energy ranging from 5-11keV below the photo peak with difference corresponding to the characteristics K X-ray energy of germanium.

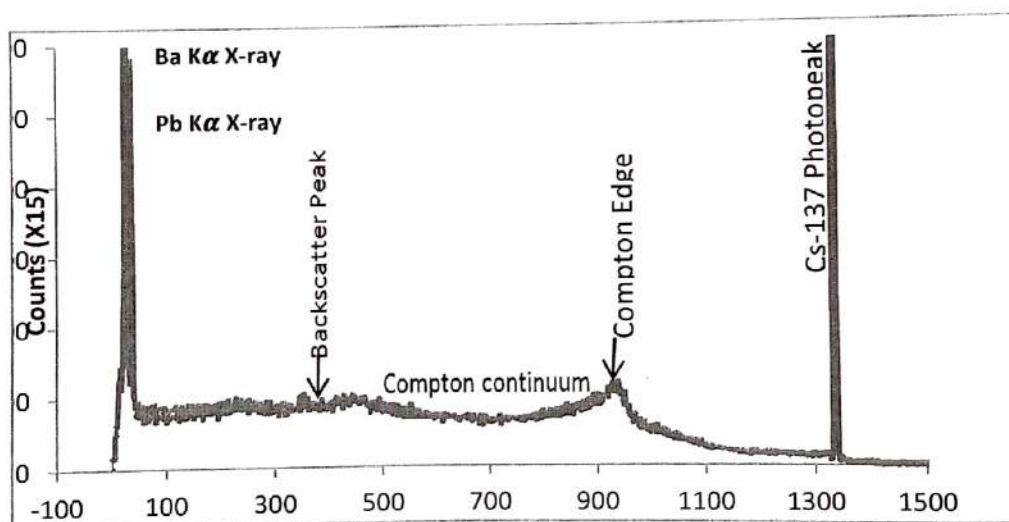
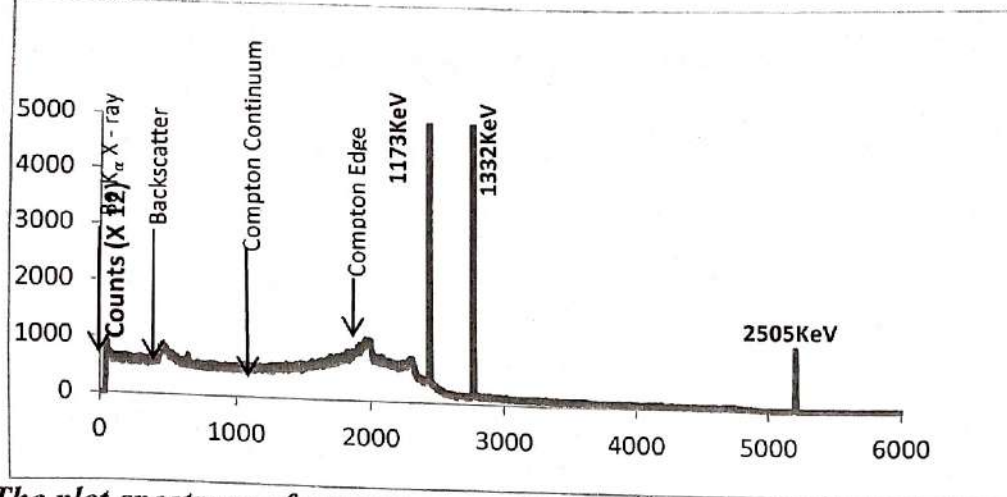


Figure 3: The spectrum plot of gamma ray emitted for source - detector distance of 200mm and 239930Bq by <sup>137</sup>Cs. Note: The scale was greatly reduced during the plot for all notable features to be pronounced.

The Calibrated spectrum of gamma ray emitted by <sup>60</sup>Co also showed all the characteristics features of Backscatter, Compton continuum, Compton edge before its full energy peaks at 1173keV,

1332KeV. Also, a single pulse sum coincidence peak of 2505.7 KeV whose amplitude corresponds to the sum of the two gamma peaks when source was taken closer to the detector(see Figure 3 and 4).



**Figure 4:** The plot spectrum of gamma ray emitted by  $^{60}\text{Co}$  20419.9Bq with source - detector distance of 200mm showing its two energy peaks and the sum peak. Note: The scale was greatly reduced during the plot for all notable features to be pronounced.

Figure 9 showed the calibrated spectrum all sources placed simultaneously at the expected energy peaks on the detector. Three full energy peaks of 662 keV for  $^{137}\text{Cs}$  and 1173 keV, 1332 keV both for  $^{60}\text{Co}$  including three additional peak energies of 511keV 1275 keV for  $^{22}\text{Na}$  and  $\text{K}\alpha$  X-ray escape Peaks. This was to explain the fact that once the MCA is calibrated, all the energy peaks of the sources will fall in line accordingly.

What facilitates the interpretation of both known and unknown gamma ray spectrum was made possible by the decay scheme (Lederer, Hollander & Perlman, 1978). Figure 4(a) and (b) shows the linearity energy response of the detector viewing from MCA and eye inspection which is an indication that the quantity of energy deposited on the detector is proportional to output pulse energy. The percentage ratio of MCA to eye inspection was 1.5% to 0.2% at energy range of 662KeV to

1332KeV which shows the accuracy of the detector since there was no significant difference when viewed in both methods.

Figure 5 shows the Energy resolution as expected from the detector under study was 0.2% at a range of both 662KeV and 1332KeV using equation 1. This confirms the good resolution of HPGe which is often determined by the inherent statistical spread in the number of charge carriers, variation of charge efficiency and contribution of electronic noise (Knoll, 2010). A gradient of  $0.69 \pm 0.8$  was obtained when a graph of  $\text{Log}E$  versus  $\text{Log}R$  was plotted confirming fluctuations that characterised Gaussian statistics. This was however at variance with gradient of equation 3 ( $1/2$  or  $0.5$ ) since there was no broadening of peak which is mostly obtained in NaI (Tl) spectrum confirming fluctuations that characterise Poisson statistics.

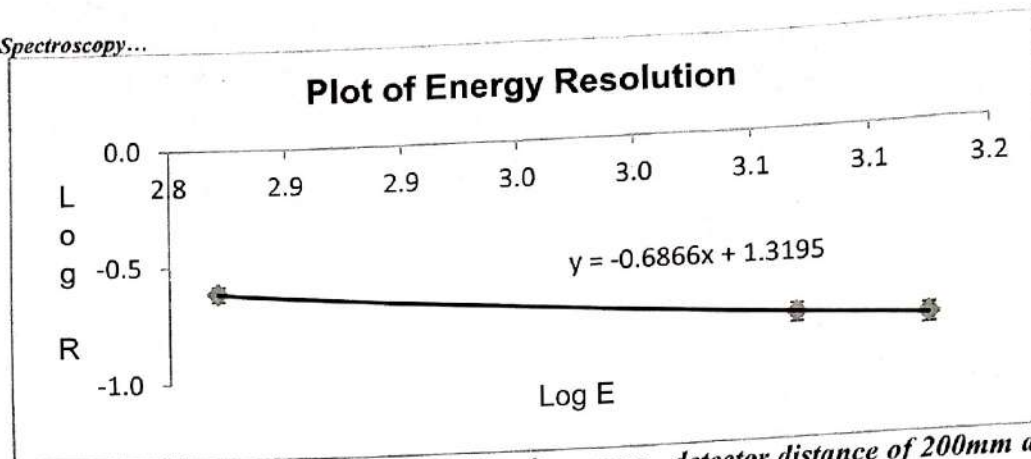


Figure 5: Plot of Energy Resolution showing gradient for source - detector distance of 200mm and 239930Bq for <sup>137</sup>Cs & 20419.9Bq for <sup>60</sup>Co. The error bars on the graph represent the all associated events of gamma yield, source-detector distance activity playing during the experiment.

The Absolute Total, Absolute Peak, Intrinsic Peak and Intrinsic Total Efficiency of the detector were determined (equation 6a, b and c). Sources information as regarding counts were obtained from their spectra, their current activities and geometry of the detector also taking into consideration. These efficiency values obtained appeared as expected when compared to the standard values.

However, it is pertinent to note that the graph of efficiency as a function of Energy (Figure 6a,b,c) did not appear exactly as compared to the standard curve because the radioactive sources given for the efficiency determination did not span across all energy levels as would be obtained in Eu-152. The But Eu-152 source given was only used for complex source analysis.

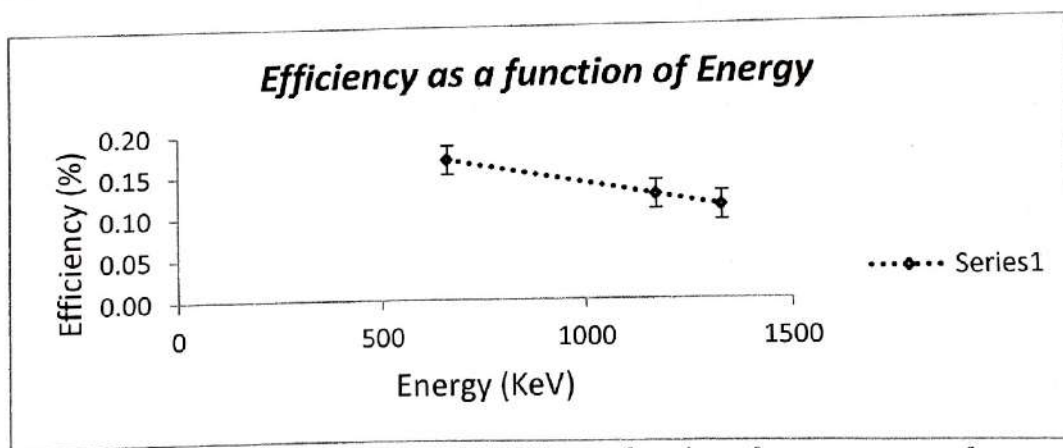


Figure 6a: Plot of ABSOLUTE TOTAL EFFICIENCY as a function of gamma energy for source - detector distance of 200mm and 239930Bq for <sup>137</sup>Cs. The error bars on the graph represent the all associated events of gamma yield, source-detector distance activity playing during the experiment.

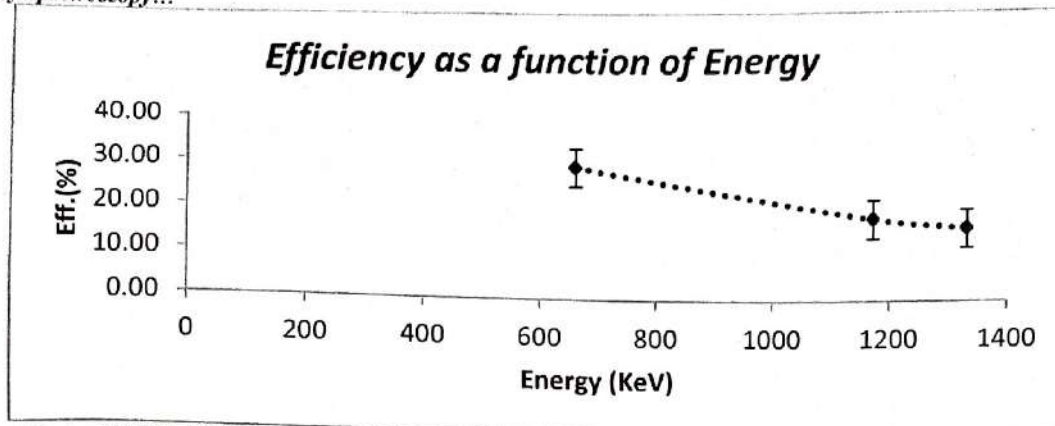


Figure 6b: Plot of **INTRINSIC PHOTOPEAK EFFICIENCY** as a function of gamma energy for source - detector distance of 200mm and 239930Bq for  $^{137}\text{Cs}$ . The error bars on the graph represent the all associated events of gamma yield, source-detector distance activity playing during the experiment.

A normal efficiency curve will always rise at about 200 keV before experiencing a linear reduction. However, as it is observed in the above two plots it only showed linear reduction in values which started

from 662KeV to 1MeV (1332KeV) as a result of photon energy of the sources used but still conforming with the characteristics of high efficiency of HPGe (Knoll, 2010).

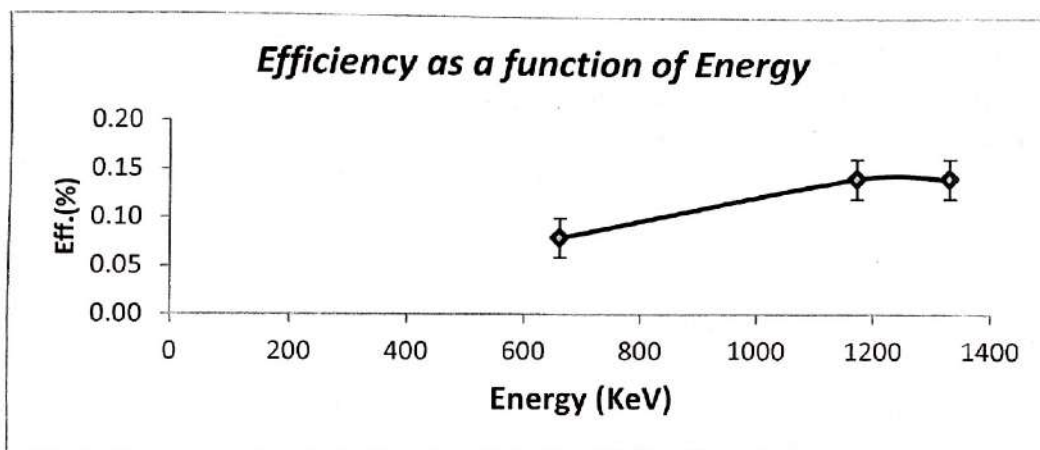


Figure 6c: Plot of **INTRINSIC TOTAL EFFICIENCY** as a function of gamma energy for source - detector distance of 200mm and 239930Bq for  $^{137}\text{Cs}$ . The error bars on the graph represent the all associated events of gamma yield, source-detector distance activity playing during the experiment.

Moreover, when attempted to calculate the Intrinsic Total Efficiency values obtained were unrealistic when compared to theoretically standard value spanning from  $(115.80 \pm 0.01)\%$  at 662KeV to  $(205.49 \pm 0.04)\%$  at 1332KeV. This great deviation was found to arise from the following factors:

- i. Uncertainties during counting due to the strength of the source are weak but quit suitable for laboratory teaching work (Appendix 7a, Table 1). It was noted that the sources acquired on December 1, 1988 (Radiation Source Data, University of Surrey) while the

half-life of  $^{60}\text{Co}$  is 5 years which its useful life has already been exceeded and  $^{137}\text{Cs}$  which is 30years and very close to end of its useful life and increasing the source strength on this particular experiment will yield better efficiency.

- ii. Source- detector distance of 200mm was too large which directly affects the percentage of the solid angle or geometry of the detector. Therefore, due to (i) above the rate at which source deposit on the detector reduces.

**Gamma – Ray Spectroscopy...**

- iii. The gamma scattering around the detector and air attenuation as well as environmental effect.

Figure 11(see Appendix) shows complex energy spectrum of Eu-152 source with Ka x-rays at energy of 39.6keV before its first notable energy peak and also photon energy ranging from 122keV to 1408keV which were all identified and labelled. Figure 12 (see Appendix) on the other hand, is a complex spectrum exhibiting an unknown source giving some names of notable gamma sources appeared on each full energy peak like 662keV belonging to  $^{137}\text{Cs}$ , 511 and 1274 keV of  $^{22}\text{Na}$ , etc which through the effect of good energy resolution of HPGe they were all identified and labelled. Also, via the good resolution, other small or narrow but tall peaks arose above the statistical noise of the continuum making it possible to identify even a weak peak superimposed on a statistically uncertain continuum (Lederer, Hollander & Perlman, 1978, Knoll, 2010).

**Recommendations**

Having studied the HPGe carefully, the following recommendations were made in order to see how the efficiency of the experimental setup can be improved.

- i. The strength of the source should be increased commensurate with the distance to the detector.
- ii. The source - detector distance should be reduced if using a weak source, to be commensurate with the source strength.
- iii. Shielding should be created around the source to minimise the gamma-ray scattering and reduced environmental interference.
- iv. Sources should be carefully selected to span across lower energy to higher energy level like Eu-152 if a good efficiency curve is expected.

**Acknowledgment**

We appreciate the contributions of the Laboratory personnel (Physic Dept. Uni-Surrey) – Gary Strudwick and Simon Banes, and the comments of Prof P.H. Regan.

**Reference**

- Ellis M. "Germanium Detection Characterisation", Spring Semester Project (Unpublished), Department of Physics, University of Surrey, (2007)
- Heath R. L. "Scintillator Spectrometry", USAEC report IDO-16880-1 (1964)
- Knoll G. F. "Radiation detection and measurement", 4<sup>th</sup> Edition. New York: John Wiley & Sons, (2010).
- Lederer G.M., Hollander J.M. and Perlman I. "Table of Isotopes" Wiley & Sons 7<sup>th</sup> Edition, (1978).
- Lilley J.S. "Nuclear Physics, Principles and Applications", New York: John Wiley & Sons, (2001).
- Slack L. and Way K. "Radiation from Radioactive Atoms" (United States Atomic Energy Commission, Washington D.C., (1959). Surrey (University of Surrey) REP 2. "Gamma-Ray Spectroscopy" (Lab Scripts), Department of Physics, University of Surrey, (2011).

Appendix

Appendix A: Tables of Values

Table 1: Source values used for calculation.

Source	E <sub>γ</sub> (KeV)	Activity (KBq) @ 01-12- 88	Activity (Bq) @ 1-12-11	C <sub>i</sub> (cps)	C <sub>p</sub> (cps)	I <sub>γ</sub> (E <sub>γ</sub> )
Cs-137	662	412	237300	536113.0±43.8	122700±20	0.85
Co - 60	1173	412	20411.2	87000±17	7594.0±5.0	1
Co - 60	1332	412	20411.2	87000±17	6717.0±4.7	1

Table 2A: Table showing calculated Energy Resolutions, Efficiencies etc.

Source	Energy	C <sub>t</sub>	C <sub>p</sub>	FWHM	N <sub>γ</sub>	N' <sub>γ</sub>	Eap(%)	Eip(%)	Resolution (%)	Eat(%)
Cs - 137	662	536113 ± 44	122700± 20	1.6	6051150	417529	0.20±.00	29.39±.00	0.24	0.09 ±6E <sup>-5</sup>
Co - 60	1173	87000± 17	7594± 5	1.9	6123360	42251	0.12±.01	17.97±.01	0.16	0.14±3E <sup>-4</sup>
Co - 60	1332	87000± 17	6717± 5	2	6123360	42251	0.11±.01	15.90±.01	0.15	0.14 ±3E <sup>-4</sup>

Table 2B

Source	Energy (KeV)	MCA	EYE	FWHM	Eit(%)
Cs - 137	662	1388	1367	1.6	128.40
Co - 60	1173	2430	2424	1.9	205.91
Co - 60	1332	2775	2764	2	205.91

Appendix B: Calibration Spectra for the MCA

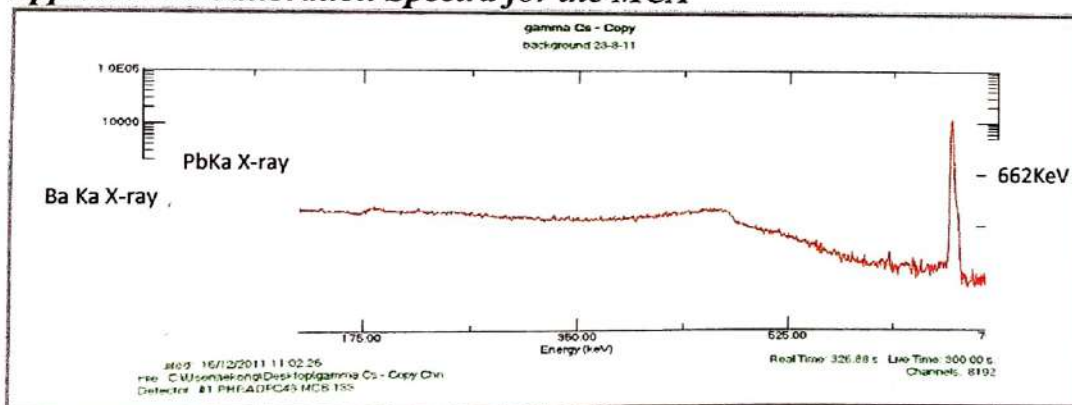


Figure 7: Calibrated Spectrum of Cs -137 showing 662KeV energy peak and Ka X-ray escape peaks of Ba at 32.1KeV and Pb at 74.2KeV.

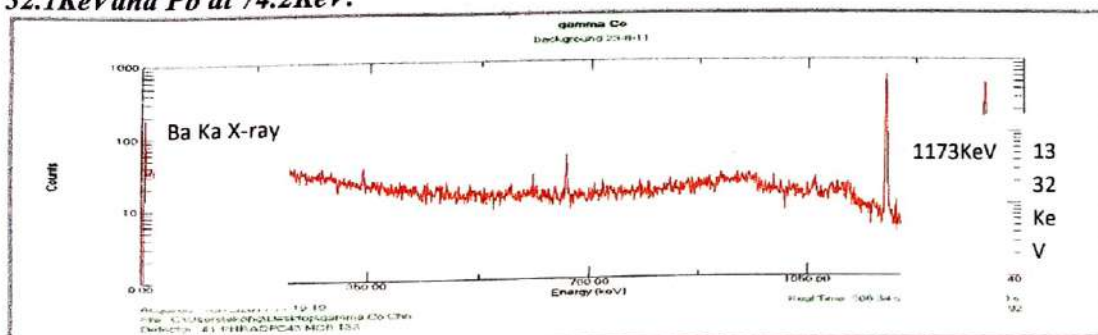


Figure 8: Calibrated Spectrum of Co - 60 showing 1173KeV and 1332KeV energy peaks and Ka X-ray escape Peaks of Ba at 32.1KeV.

Measurement of Planck's constant base ...

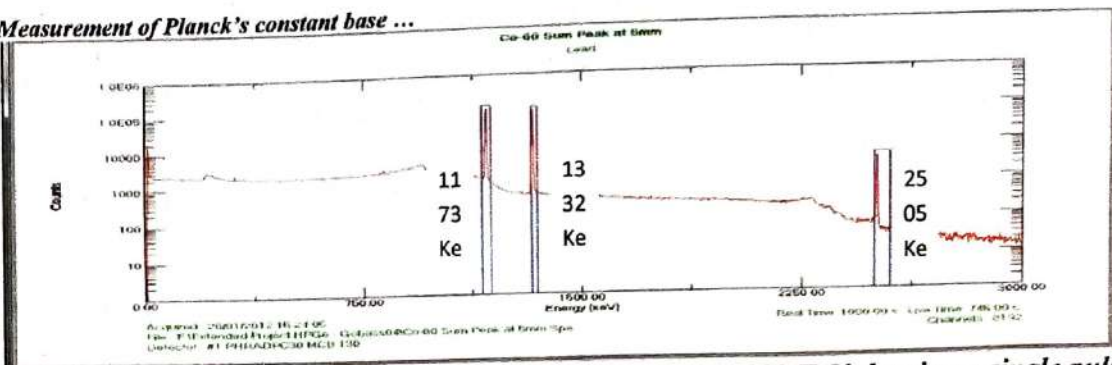


Figure 9: Calibrated Spectrum of Co – 60 at 1173 KeV and 1332 KeV showing a single pulse sum coincidence peak of 2505.7 KeV whose amplitude corresponds to the sum of the two gamma peaks when source was taken closer to the detector.

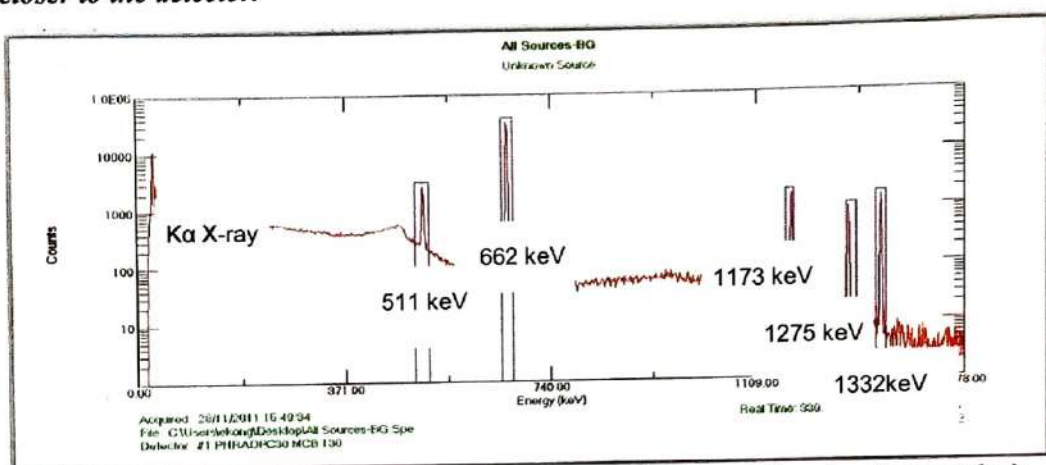


Figure 10: Calibrated spectrum showing all sources placed the simultaneously in the detector. Three full energy peaks of 662keV for <sup>137</sup>Cs, 1173keV and 1332keV both for <sup>60</sup>Co included three additional peak energies of 511keV 1275keV for <sup>22</sup>Na and Ka X-ray escape Peaks were observed.

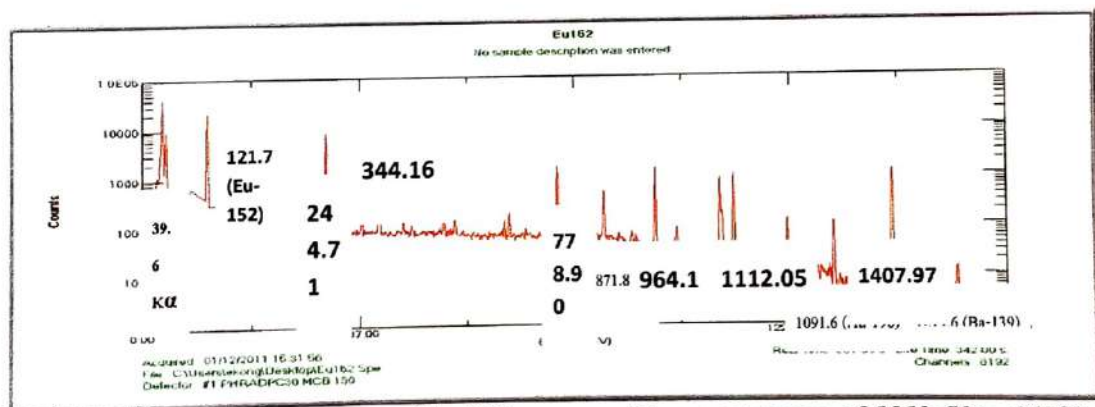


Figure 11: Complex Spectrum of Eu-152 source with energy range of 121keV to 1458keV with Ka x-rays at energy of 39.6keV

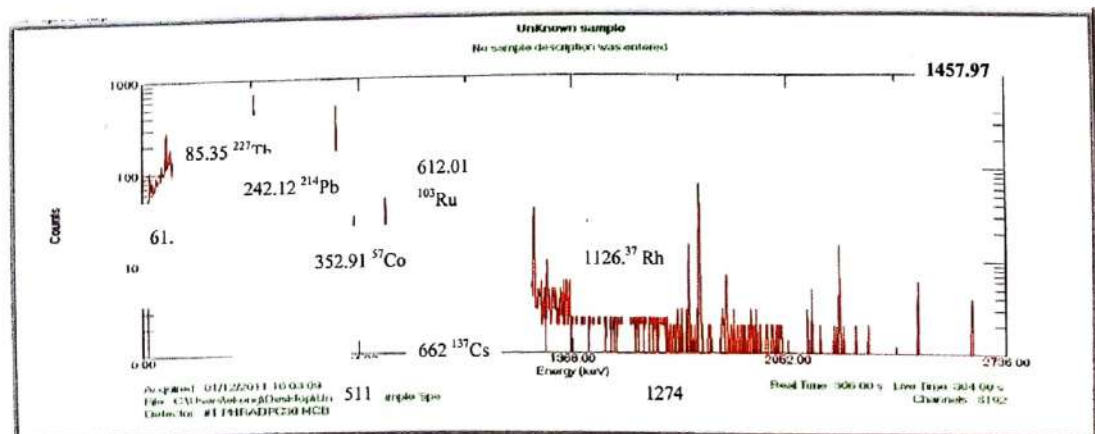


Figure 12: Complex spectrum of Unknown Source sample